

Signatures of Lévy flights with annealed disorder

Q. Baudouin¹, R. Pierrat², A. Eloy¹, E.J. Nunes-Pereira³, P.-A. Cuniasse², N. Mercadier^{1,†}, and R. Kaiser¹

¹*Université de Nice Sophia Antipolis, CNRS, Institut Non-Linéaire de Nice, UMR 7335, F-06560 Valbonne, France*

²*Institut Langevin, ESPCI ParisTech, CNRS, 1 rue Jussieu, 75238 Paris Cedex 05, France*

³*Department of Physics and Center of Physics, University of Minho, 4710-057 Braga, Portugal*

[†]*Now at Saint-Gobain Recherche, 39 Quai Lucien Lefranc, 93303 Aubervilliers, France*

(Dated: February 26, 2014)

We present theoretical and experimental results of Lévy flights of light originating from a random walk of photons in a hot atomic vapor. In contrast to systems with quenched disorder, this system does not present any correlations between the position and the step length of the random walk. In an analytical model based on microscopic first principles including Doppler broadening we find anomalous Lévy-type superdiffusion corresponding to a single-step size distribution $P(x) \propto x^{-(1+\alpha)}$, with $\alpha \approx 1$. We show that this step size distribution leads to a violation of Ohm's law [$T_{\text{diff}} \propto L^{-\alpha/2} \neq L^{-1}$], as expected for a Lévy walk of independent steps. Furthermore the spatial profile of the transmitted light develops power law tails [$I(r) \propto r^{-3-\alpha}$]. In an experiment using a slab geometry with hot rubidium vapor, we measured the total diffuse transmission T_{diff} and the spatial profile of the transmitted light $I(r)$. We obtained the microscopic Lévy parameter α under macroscopic multiple scattering conditions paving the way to investigation of Lévy flights in different atomic physics and astrophysics systems.

PACS numbers: 05.40.Fb, 11.80.La, 05.60.Cd, 42.25.Bs, 42.25.Dd

Transport of waves in complex media has been studied for many decades, even though many fundamental or applicative questions are still under debate such as imaging through optical thick samples [1] or Anderson localization [2]. Light propagation in turbid media can often be described by a diffusion formalism where photons undergo a random walk process with a step-size distribution $P(x)$ vanishing faster than $1/x^3$ at infinity. In that case the central limit theorem applies and the mean-square displacement of photons is proportional to time. This is typically the case for light in cloudy atmospheres [3] or in biological tissues [4].

However, many physical systems can be subdiffusive or superdiffusive depending on the random walk process characteristics. One particular mechanism for superdiffusion is called Lévy flights. The occurrence of Lévy flights has been investigated in a large variety of systems, ranging from trajectories of animals [5, 6], human travel [7, 8], turbulence [9], earthquakes [10] to solar flares [11]. In optics, engineered materials where photons trajectories are described by Lévy flights have been realized recently by stacking glass spheres with a specific size distribution (and are thus called Lévy glasses) [12, 13]. In many of these systems, as in most turbid media relevant in applied physics [14], possible correlations exist between the step-size distribution and the initial position of the step depending on the underlying topography of the system (e.g. quenched disorder in Lévy glasses) [15]. These correlations are at the root of some limitations in the observation of Lévy flights characteristics [16], and it is thus important to look for a system without any of such correlations.

As suggested early on by Kenty [17] and reformulated later in the context of Lévy flights [18], superdiffusion of

light is also expected in many different atomic systems ranging from dense atomic vapors, hot plasmas to stars. In this Letter, we explore theoretically, numerically and experimentally the propagation of light in a slab containing a hot rubidium gas. This system corresponds to an annealed disorder where no correlation exists between the step-size distribution and the position [16]. Furthermore, the range of step-size distribution in atomic vapors is only limited by nearest neighbor distances and by the size of the sample, allowing for a huge increase in the dynamics of the signals. Previous theoretical work on Lévy flights of light have already been conducted in atomic vapors but are fully phenomenological [18, 19].

In our theoretical approach, we derive a transport equation from first principles (microscopic approach starting from Maxwell equations) and with controlled approximations. This equation describes the incoherent propagation of radiation inside a gas consisting of two-level atoms at high temperature. Solving this integro-differential equation using a Monte Carlo technique allows us to obtain both the total diffuse transmission T_{diff} as well as the intensity profile $I(r)$ at the exit surface of the sample. A careful analytical analysis of the integro-differential equation also leads us to an analytical expression for the step-size distribution $P(x)$, which we use to obtain analytical prediction for the power law decrease of $I(r)$ which is directly related to the Lévy exponent α .

In an experiment using a slab geometry with hot rubidium atoms, we have measured the total diffuse transmission T_{diff} and the transmitted intensity profile $I(r)$, both in excellent agreement with the theoretical predictions. The large dynamic range of the experiment data provides a reliable measurement for the Lévy exponent α , measured in single shot images under multiple scat-

tering conditions and is very close to the result obtained in a previous study based on the microscopic step-size distribution of light in the system [20].

We start the derivation of the transport equation for light in atomic clouds with the polarizability of the atoms described by $\alpha(\delta) = -4\pi/k_0^3 [i + 2\delta/\Gamma]^{-1}$ where $\delta = \omega - \omega_0$ is the detuning, ω_0 being the resonance frequency, Γ the linewidth and $k_0 = \omega_0/c_0$ the wavevector. This expression is valid for a two-level atom far from saturation and does not take into account the multilevel structure of the real atoms considered in the experiment. From this building block and from first principles (Maxwell equations), we derive a transport equation valid for a dilute gas at any temperature. It reads in the temporal Fourier space (see Ref. [21] for more details)

$$\begin{aligned} & \left[-i\frac{\Omega}{c_0} + \mathbf{u} \cdot \nabla_{\mathbf{r}} + \int \mu_e(\delta - k_0 \mathbf{u} \cdot \mathbf{v}, \Omega) g(\mathbf{v}) d\mathbf{v} \right] \\ & \times I(\mathbf{u}, \mathbf{r}, \delta, \Omega) = \frac{1}{4\pi} \int \mu_s(\delta - k_0 \mathbf{u} \cdot \mathbf{v}, \Omega) \\ & \times I(\mathbf{u}', \mathbf{r}, \delta + k_0(\mathbf{u}' - \mathbf{u}) \cdot \mathbf{v}, \Omega) g(\mathbf{v}) d\mathbf{u}' d\mathbf{v} \quad (1) \end{aligned}$$

where I is the specific intensity (local radiative flux at position \mathbf{r} , direction \mathbf{u} , frequency δ and time t , Ω being the Fourier variable for time). $g(\mathbf{v})$ is the atomic velocity distribution with mean-square \bar{v} (gaussian profile). Equation (1) is close to the standard Radiative Transfer Equation (RTE) [22] except that temporal convolution products and frequency shifts are present to take into account atomic resonances and Doppler effects (finite temperature) respectively. The extinction and scattering coefficients are given by $\mu_e(\delta, \Omega) = -i\rho k_0/2 [\alpha(\delta + \Omega/2) - \alpha^*(\delta - \Omega/2)]$ and $\mu_s(\delta, \Omega) = \rho k_0^4/(4\pi)\alpha(\delta + \Omega/2)\alpha^*(\delta - \Omega/2)$ where ρ is density of atoms. These expressions ensure energy conservation (the optical theorem is fulfilled). The domain of interest was previously cold atoms where $k_0\bar{v}/\Gamma \ll 1$ [21]. In the case of hot atomic vapors, the Doppler shift is larger than the natural linewidth. Thus we have to take the limit of Eq. (1) when $k_0\bar{v}/\Gamma \gg 1$. In practice, we also perform a long time approximation by considering $\Omega \ll \delta, \Gamma, k_0\bar{v}$. We obtain (see Sec. 1 of supplementary material)

$$\begin{aligned} & \left[\mathbf{u} \cdot \nabla_{\mathbf{r}} + \left(1 + \frac{1}{\Gamma} \frac{\partial}{\partial t} \right) \mu_l(\delta) \right] I(\mathbf{u}, \mathbf{r}, \delta, t) \\ & = \frac{\mu_l(\delta)}{4\pi} \int p(\delta, \delta', \mathbf{u}, \mathbf{u}') I(\mathbf{u}', \mathbf{r}, \delta', t) d\mathbf{u}' d\delta' \quad (2) \end{aligned}$$

where the extinction coefficient reduces to $\mu_l(\delta) = \Gamma/(2\ell_0 k_0 \bar{v}) \sqrt{\pi/2} \exp[-\delta^2/(2k_0^2 \bar{v}^2)]$ with ℓ_0 the scattering mean-free path for pinned atoms at resonance. The scattering coefficient reduces to $\mu_l p(\delta, \delta', \mathbf{u}, \mathbf{u}')$ where p

is the phase function (frequency redistribution) given by

$$\begin{aligned} p(\delta, \delta', \mathbf{u}, \mathbf{u}') &= \frac{1}{\sqrt{2\pi} k_0 \bar{v} \sqrt{1 - (\mathbf{u} \cdot \mathbf{u}')^2}} \\ &\times \exp \left[-\frac{(\delta' - \delta \mathbf{u} \cdot \mathbf{u}')^2}{2k_0^2 \bar{v}^2 (1 - (\mathbf{u} \cdot \mathbf{u}')^2)} \right] \quad (3) \end{aligned}$$

This expression shows that frequency redistribution is not complete at each scattering event. The scattered frequency is still related to the incident one through the scattering angle given by $\mathbf{u} \cdot \mathbf{u}'$. Please note that a similar equation to Eq. (2) was derived previously in the steady-state regime in the context of planetary nebula [23].

First, we solved Eq. (2) using an exact Monte Carlo scheme and we obtained the transmitted intensity profile $I(r)$ for a sample in the multiple scattering limit. As shown in Fig. 2 (d), the wings of the profile develop a well pronounced power law, in contrast to the wings obtained in the classical diffusive limit, where this profile has an exponential tail (see Sec. 3 supplementary material).

To go further with an analytical approach and show that Lévy flights are encoded in this equation, we need to perform the approximation $\mathbf{u} \cdot \mathbf{u}' = 0$. This assumption is true on average (isotropic scattering) and holds only if a large number of scattering events are encountered by photons before leaving the system (validity checked numerically by Monte Carlo simulations). It implies complete frequency redistribution. In the following, we also consider a 3D slab geometry of thickness L along direction z . In that case, by integrating Eq. (2) over the azimuthal angle φ , we obtain

$$\begin{aligned} & \left[\mu \frac{\partial}{\partial z} + \left(1 + \frac{1}{\Gamma} \frac{\partial}{\partial t} \right) \mu_l(\delta) \right] I(\mu, z, \delta, t) \\ & = \frac{\mu_l(\delta)}{2} \int_{-\infty}^{\infty} p(\delta') I(\mu', z, \delta', t) d\mu' d\delta' \quad (4) \end{aligned}$$

where $p(\delta') = \exp[-\delta'^2/(2k_0^2 \bar{v}^2)] / (\sqrt{2\pi} k_0 \bar{v})$ and $\mu = \cos \theta$, θ being the polar angle between the direction \mathbf{u} and the axis z . This equation allows us to derive the expression of the step-size distribution and to compute analytically its asymptotic behavior given by

$$P(x) = \int \mu_l(\delta) \exp[-\mu_l(\delta)x] p(\delta) d\delta \propto 1/x^{(\alpha+1)} \quad (5)$$

when $x \rightarrow \infty$ with $\alpha = 1$. In this limit the average and the variance of the scattering length are not defined, leading to a diverging diffusion coefficient, confirming the presence of Lévy flights induced by large Doppler shifts (high temperature) in conjunction with sharp resonances (high quality factor of the atomic transition).

Performing a modal expansion of the specific intensity (spatial Fourier transform combined with temporal eigenmodes [21, 24]), one can obtain further analytical

predictions and derive the dispersion relation of Eq. (4). It writes in the form (see Sec. 2 of supplementary material) $s(k)/\Gamma \propto k^\alpha$ when $k \rightarrow 0$, k being the Fourier variable for space. $s(k)$ is the temporal decay rate of the specific intensity for mode k , leading to a time decay scaling for large times as

$$I(t) \propto \exp\left[-a \frac{t}{L^\alpha}\right], \quad (6)$$

where a is a coefficient independent of the sample thickness L . This could be observed in time resolved experiments.

This dependence on k^α for large systems (small k) confirms again the presence of Lévy flights and leads to an anomalous diffusion equation with a spatial derivative $\Delta^{\alpha/2}$ where $\alpha = 1$ [25]. From a random walk point of view, it has also been shown that the asymptotic scaling $P(x) \propto 1/x^{\alpha+1}$ of the step-size distribution of independent steps implies a power law behavior for the steady-state total diffuse transmission $T_{\text{diff}} \propto L^{-\alpha/2}$ at large optical thicknesses [12, 26]. We have exploited Eq. (5) further and shown analytically that, assuming the last step to be the dominant contribution, the transmitted intensity profile $I(r)$ has power law tails which scale as (see Sec. 3 of supplementary material)

$$I(r) \propto r^{-3-\alpha}. \quad (7)$$

Indeed, we assume that photons escaping the system in transmission very far from the laser axis (tail of the radial profile, i.e. $r \gg L$) undergo a very long last step leading to neglect all other steps. Considering that this last step is described by $P(x) \propto 1/x^{\alpha+1}$, we find the correct behavior for the tail of the radial profile. The tails of the transmitted intensity profile can thus be used to measure the Lévy exponent α , even if no microscopic model from first principles is available. We stress that the possibility to extract the Lévy exponent from one single transmission profile has an important advantage, as one does not need to realize samples with different size or opacity, already often difficult in laboratory environment, but impossible to realize in the astrophysical context.

Experimentally, microscopic measurements of the step-size distribution have already been realized [20] showing the existence of Lévy flights of light in hot atomic vapors. In this Letter, we focus on the macroscopic evidence of Lévy flights by recovering the Lévy parameter α using a stationary experiment under multiple scattering conditions. Our experiment is really close to ideal Gedanken experiment. We illuminate a flat cell of thickness $L = 3$ mm filled with a rubidium vapor. We control the density of atoms by adjusting the temperature of the cell ranging from 40 °C (room temperature) to 170 °C. This corresponds to a change in opacity O from 10^2 to 10^5 where $O = L/\ell_0$, ℓ_0 being the scattering mean-free path

at resonance for pinned atoms (if they had no Doppler broadening). The opacity O is a more accurate measure of the effective thickness of the sample L but the scaling laws for O and L are identical. Experimentally, the opacity O is estimated by measuring the coherent transmission T of a laser beam. The incident frequency is tuned to scan all D2 lines of two rubidium isotopes (^{85}Rb and ^{87}Rb , see Fig. 1(b) and Sec. 4 of supplementary material). In our range of temperature, the opacity scales as $O \sim -200 \log(T)$ which ensures the multiple scattering regime. The spectral broadening is proportional to the square root of the temperature while the vapor pressure depends exponentially on the temperature ensuring that the Doppler effect is almost not affected by the temperature.

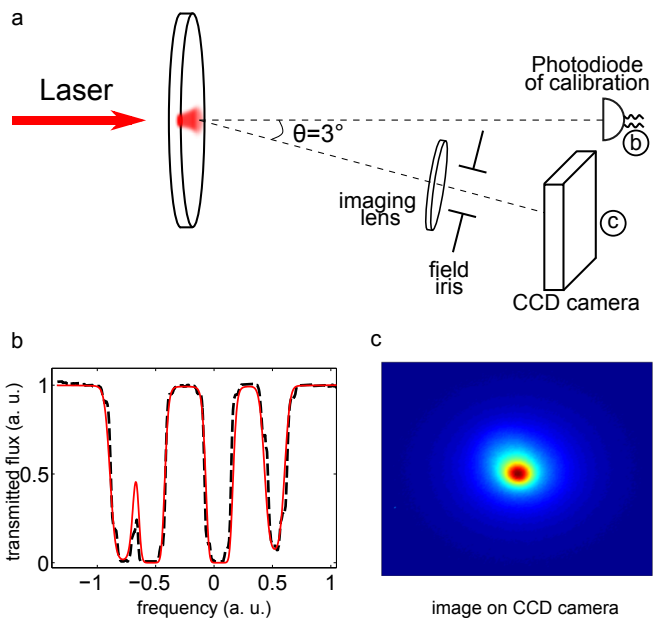


FIG. 1: (Color online) (a) Experimental setup: A laser beam is incident on a flat cylindrical cell filled with a rubidium vapor. The transmitted ballistic light spectrum is measured via a photodiode aligned with the laser beam. The scattered light coming out of the slab is imaged on the CCD camera misaligned by an angle of 3° with the laser. (b) Signal of the photodiode: The transmission of the laser scanned in frequency throughout the rubidium cell shows the D2 hyperfine absorption of ^{85}Rb and ^{87}Rb . An ab-initio fit of this signal is used to deduce the opacity O (see Sec. 4 of supplementary material). (c) Image of the radial profile observed on the CCD camera.

For long term stability and an absolute frequency reference we lock the laser on the $F = 2 \rightarrow F' = 2 - F' = 4$ crossover of the D2 line of ^{85}Rb . We image the outgoing flux on a CCD camera via a lens of 50 mm of focal length [see Fig. 1(a)]. To improve the signal-to-noise ratio and to have access to a good accuracy in the tail of the radial profile $I(r)$, we perform an angular average by adding

36 slices (separated by an angle of 10° from each other).

In Fig. 2(b) we plot the total transmission incoming on all pixels of the CCD camera as a function of the opacity. We clearly see that the total transmission T_{diff} does not scale as Ohm's law prediction (i.e. $T_{\text{diff}} \propto O^{-1}$) but has a superdiffusive behavior (i.e. $T_{\text{diff}} \propto O^{-0.516}$), in excellent agreement with the prediction at large opacities $T_{\text{diff}} \propto O^{-\alpha/2}$ for $\alpha \approx 1$ [12, 26]. Considering the single step size distribution measured in [20] this exponent is in excellent agreement with the expectation for the total diffuse transmission for a Lévy walk of independent steps and different from random walk in quenched disorder [16].

Exploiting the excellent signal to noise ratio of our angular averaged CCD images, we also plot the radial profile of the transmitted intensity $I(r)$ in linear [see Fig. 2(c)] and logarithmic [see Fig. 2(d)] scales, highlighting the large dynamic range of our signal. We clearly see that the general shape is far from a gaussian profile. We note that even in the diffusive limit, the transmitted profile is not gaussian shape, but develops exponential tails (see Sec. 3 of supplementary material for theory and experiments). In the Lévy flight regime however, the tail clearly exhibits a power law: $I(r) \propto r^{-4.03 \pm 0.15}$, as predicted by Eq. (7) for $\alpha = 1.03 \pm 0.15$. Moreover, this asymptotic behavior is valid for a wide range of opacities as shown on Fig. (3). We note that for increasing opacity, the total relevant signal is reduced [see Fig. 2(b)] and the relative importance of amplified spontaneous emission pedestal (see supplementary information) increases, requiring thus to adapt the range of radial distances where a reasonable fit can be obtained. Finally, we stress that the scaling laws in the tail of $I(r)$ can be obtained from a single image on the CCD, giving access to Lévy parameter with a single snapshot whose duration is 2 ms. This has to be compared to previous studies where the Lévy parameter were extracted in 30 h [27]. Also, with only one snapshot, the vertical dynamics is more than four orders of magnitude and allow a good fit. Furthermore, this single image under multiple scattering condition allows to make use of this scaling laws in different experimental conditions, in laboratory environment or in astrophysical systems.

One interesting point concerning the radial profile is the behavior at small distances r . In Lévy glasses [12], a pronounced cusp is observed close to $r = 0$ which is not the case neither in our experiment nor in simulations. There are several fundamental differences between Lévy glasses and hot atomic vapors illuminated by a monochromatic laser beam. For Lévy glasses, when light enters the system, the step-size distribution is already a power law with an exponent $\alpha < 2$ leading to superdiffusion. In our hot vapor experiment in contrast, the correct step-size distribution for photons at the laser frequency is an exponential function $\mu_l(\delta_0) \exp[-\mu_l(\delta_0)x]$, different from the power law step-size distribution after one

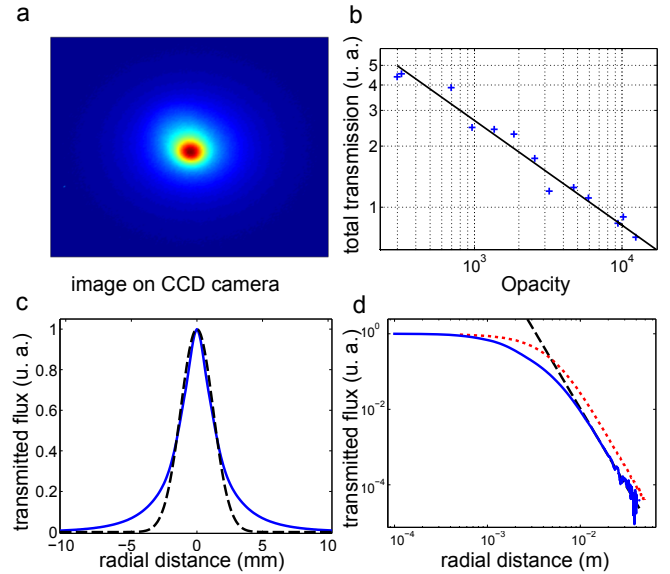


FIG. 2: (Color online) (a) Image of the radial profile on the CCD camera. (b) Blue crosses: Experimental total transmission (in log scale) as a function of the opacity. Each point corresponds to the sum of all pixels of a CCD image for a given opacity. Black solid line: fit of the experimental data. The power law obtained is $T_{\text{diff}} \propto O^{-0.516 \pm 0.024}$. (c) Blue solid line: Experimental radial profile (in linear scale) of the scattered light transmitted through the cell. Black dashed line: Gaussian profile with the same width at half maximum as the experimental profile. (d) Blue solid line: Experimental radial profile (in log scale) of the scattered light transmitted through the cell. Dotted red line: Numerical prediction from a Monte Carlo simulation of the transport equation. Black dashed line: fit of the experimental data in the range $[1.1, 2.1]$ cm. The power law obtained is $I(r) \propto r^{-4.03 \pm 0.15}$. The temperature is $T = 114^\circ\text{C}$ corresponding to an opacity of $O = 1.15 \cdot 10^4$ and an optical thickness of $b = 540$.

scattering event, where the frequency is already redistributed. We have checked numerically that if a broadband excitation were used to illuminate the hot atomic vapor cell, a sharp cusp around the center of the transmitted light path is recovered.

In summary, we have shown theoretical, numerical and experimental results confirming Lévy flights of photons in hot vapor under multiple scattering condition with annealed disorder. Lévy flights in our system appear due to the interplay between the high quality factor of atomic resonances and large Doppler broadening. The scaling laws obtained for the diffuse transmission T_{diff} and intensity profile $I(r)$ suggests that other spectral broadenings such as collisions with a buffer gas could allow to enhance or control Lévy flights and will be accessible in realistic experimental conditions. This work opens also new perspectives to look for evidence of Lévy flight in astrophysical systems or for quantitative studies of the limits of validity of the complete frequency redistribution in hot vapors.

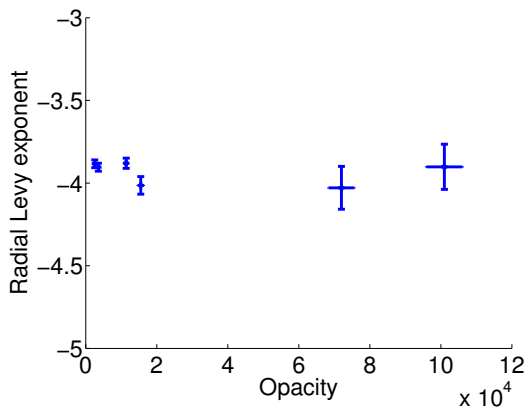


FIG. 3: (Color online) Power law exponent of the radial profile tail of the transmitted intensity $I(r)$ as a function of the opacity O tuned by varying the temperature. This exponent is close to -4 for a wide range of opacity showing the robustness of the Lévy character of the system. Vertical error bars correspond to standard deviation of the fit to extract the power law of $I(r)$. Error bars increase for large opacities due to the decrease of the relevant signal.

We thank Dominique Delande for fruitful discussions and we acknowledge funding for N.M. and Q.B. by the french Direction Générale de l'Armement. This work was supported by LABEX WIFI (Laboratory of Excellence ANR-10-LABX-24) within the French Program "Investments for the Future" under reference ANR-10-IDEX-0001-02 PSL*. E.J.N. acknowledges FCT (441.00 CNRS).

-
- [1] P. Sebbah, *Waves and Imaging through Complex Media* (Kluwer Academic, Dordrecht, 2001).
 - [2] P. Anderson, Phys. Rev. **109**, 1492 (1958).
 - [3] G. E. Thomas and K. Stamnes, *Radiative Transfer in the Atmosphere and Ocean* (University Press, Cambridge, 1999).
 - [4] V. Tuchin, Physics - Uspekhi **40**, 495 (1997).
 - [5] G. M. Viswanathan, V. Afanasyev, S. V. Buldyrev, E. J. Murphy, P. A. Prince, and H. E. Stanley, Nat. **427**, 413 (1996).
 - [6] A. M. Edwards, R. A. Philipps, N. W. Watkins, M. P.

- Freeman, E. J. Murphy, V. Afanasyev, S. V. Buldyrev, M. G. E. da Luz, E. P. Raposo, H. E. Stanley, et al., Nat. **449**, 1044 (2007).
- [7] D. Brockmann, L. Hufnagel, and T. Geisel, Nat. **398**, 462 (2006).
- [8] M. C. González, C. A. Hidalgo, and A.-L. Barabási, Nat. **453**, 779 (2008).
- [9] M. F. Shlesinger, B. J. West, and J. Klafter, Phys. Rev. Lett. **58**, 1100 (1987).
- [10] Á. Corral, Phys. Rev. Lett. **97**, 178501 (2006).
- [11] M. Baiesi, M. Paczuski, and A. L. Stella, Phys. Rev. Lett. **96**, 051103 (2006).
- [12] P. Barthélemy, J. Bertolotti, and D. S. Wiersma, Nature **453**, 495 (2008).
- [13] J. Bertolotti, K. Vynck, L. Pattelli, P. Barthélemy, S. Lepri, and D. S. Wiersma, ADVANCED FUNCTIONAL MATERIALS **20**, 965 (2010).
- [14] T. Svensson, K. Vynck, M. Grisi, R. Savo, M. Buresi, and D. S. Wiersma, Phys. Rev. E **87**, 022120 (2013), URL <http://link.aps.org/doi/10.1103/PhysRevE.87.022120>.
- [15] P. Barthélemy, J. Bertolotti, K. Vynck, S. Lepri, and D. S. Wiersma, Phys. Rev. E **82**, 011101 (2010).
- [16] C. W. Groth, A. R. Akhmerov, and C. W. J. Beenakker, Phys. Rev. E **85**, 021138 (2012), URL <http://link.aps.org/doi/10.1103/PhysRevE.85.021138>.
- [17] C. Kenty, Phys. Rev. **42**, 823 (1932).
- [18] E. Pereira, J. M. G. Martinho, and M. N. Berberan-Santos, Phys. Rev. Lett. **93**, 120201 (2004).
- [19] T. Holstein, Phys. Rev. **72**, 1212 (1947).
- [20] N. Mercadier, W. Guerin, M. Chevrollier, and R. Kaiser, Nat. Phys. **5**, 602 (2009).
- [21] R. Pierrat, B. Grémaud, and D. Delande, Phys. Rev. A **80**, 013831 (2009).
- [22] S. Chandrasekhar, *Radiative Transfer* (Dover, New-York, 1950).
- [23] W. Unno, Publ. Astron. Soc. Jap. **3**, 158 (1952).
- [24] R. Pierrat, J. J. Greffet, and R. Carminati, J. Opt. Soc. Am. A **23**, 1106 (2006).
- [25] R. Metzler, E. Barkai, and J. Klafter, Physica A: Statistical Mechanics and its Applications **266**, 343 (1999), ISSN 0378-4371, URL <http://www.sciencedirect.com/science/article/pii/S0378437198006141>.
- [26] A. Davis and A. Marshak, *Lévy kinetics in slab geometry: scaling of transmission probability*, in *Fractal Frontiers*, Eds. M.M. Novak, T.G. Dewey, World Scientific (World Scientific, Singapore, 1997), p. 63.
- [27] N. Mercadier, M. Chevrollier, W. Guerin, and R. Kaiser, Phys. Rev. A **87**, 063837 (2013).